Shortened G1 phase of cell cycle and decreased histone H3K27 methylation are associated with AKT - induced enhancement of primordial germ cell reprogramming

doi: 10.1111/dgd.12621

Shortened G1 phase of cell cycle and decreased histone H3K27 methylation are associated with AKT-induced enhancement of primordial germ cell reprogramming

Running title

PGC reprogramming by AKT activation

Asuka Takehara[1,2,4] and Yasuhisa Matsui[1,2,3,4,5]

[1]Cell Resource Center for Biomedical Research, Institute of Development, Aging and Cancer (IDAC), Tohoku University, Sendai, Miyagi, Japan

[2]Graduate School of Life Sciences, Tohoku University, Sendai, Miyagi, Japan

[3]Graduate School of Medicine, Tohoku University, Sendai, Miyagi, Japan

[4]The Japan Agency for Medical Research and Development-Core Research for Evolutional Science and Technology (AMED-CREST), Chuo-ku, Tokyo, Japan

[5]Corresponding author:

Postal address; Cell Resource Center for Biomedical Research, Institute of Development, Aging and Cancer (IDAC), Tohoku University, 4-1 Seiryo-machi, Aoba-ku, Sendai, Miyagi 980-8575, Japan

e-mail; yasuhisa.matsui.d3@tohoku.ac.jp

Phone; +22-717-8571

Fax; +22-717-8573

Abstract

Primordial germ cells (PGCs) are reprogrammed into pluripotent embryonic germ cells (EGCs) under specific culture conditions, but the detailed mechanisms of PGC reprogramming have not yet been fully clarified. Previous studies have demonstrated that AKT, an important intracellular signaling molecule, promotes reprogramming of PGCs into EGCs. Because AKT likely inhibits p53 functions to enhance PGC reprogramming, and p53 negatively regulates cell cycle progression, we analyzed cell cycle changes in PGCs following AKT activation, and found that the ratio of PGCs in the G1/G0 phase was decreased while that of PGCs in the G2/M phase was increased after AKT activation. We also showed that the expression of the CDK inhibitor $p27^{kip1}$, which prevents the G1-S transition and is transcriptionally repressed by p53, was significantly down-regulated by AKT activation. The results suggested that the characteristic cell cycle changes of PGCs by AKT activation are, at least in part, due to decreased expression of $p27^{kip1}$. We also investigated changes in histone H3K27 tri-methylation (H3K27me3) by AKT activation in PGCs, because we previously found that decreased H3K27me3 was involved in PGC reprogramming via upregulation of cyclin D1. We observed that AKT activation in PGCs resulted in H3K27 hypomethylation. In addition, DZNeP, an inhibitor of the H3K27 trimethyl transferase Ezh2, stimulated EGC formation. These results together suggested that AKT activation promotes G1-S transition and downregulates H3K27me3 to enhance PGC reprogramming.

Key words

Primordial germ cell, EG cell, pluripotent stem cell, cell-cycle, AKT, H3K27me3

Introduction

During mouse embryogenesis, the fertilized egg first develops to pre-implantation blastocysts containing the inner cell mass (ICM), which is a pluripotent stem cell cluster, and further develops to epiblasts after implantation. Under specific culture conditions, the ICM can grow and give rise to pluripotent embryonic stem cells (ESCs). In early post-implantation embryos at E (embryonic day) 7.25, germ cells emerge as primordial germ cells (PGCs), which are precursors of gametes (Ginsberg et al., 1990), and are the only cells that can pass genetic information to successive generations. PGCs normally give rise only to gametes, but are also easily reprogrammed to pluripotent stem cells either under specific culture conditions (Matsui et al., 1992, Resnick et al., 1992) or in specific genetic backgrounds (Stevens, 1973). PGC-derived pluripotent stem cells in culture, namely embryonic germ cells (EGCs), show similar cellular characteristics as ESCs.

It previously has been reported that activation of AKT, an important intracellular signaling molecule, promotes reprogramming of PGCs to EGCs (Kimura et al., 2008). AKT functions to

transmit intra-cellular signals from cytokine/growth factor receptors and affects a variety of physiological phenomena such as cell differentiation, proliferation, survival, and protein synthesis; these effects are mediated by phosphorylation of downstream target molecules (Brazil et al., 2004). In PGCs, AKT contributes to the transmission of leukemia inhibitory factor (LIF) and basic fibroblast growth factor (bFGF) signals (Kimura et al., 2008; Matsui et al., 2014). AKT may also inactivate the tumor suppressor protein p53 (Kimura et al., 2008), which generally represses cell cycle progression through transcriptional activation of genes encoding cyclin-dependent kinase inhibitors (CDKIs) such as $p21^{cip1}$ (El-Deiry et al., 1993). During the cell cycle, CDK4 / cyclin D and CDK2 / cyclin E complexes promote G1-S progression, while $p21^{cip1}$ and $p27^{kip1}$ repress G1-S transition via inhibition of the CDK / cyclin complexes (Abukhdeir and Park, 2008). $p21^{cip1}$ and $p27^{kip1}$ are involved in mitotic arrest of PGCs and are down-regulated in *Dnd1*-deficient germ cells in embryonic testes in the 129 genetic background (Cook et al., 2011); these *Dnd1*-deficient germ cells undergo reprogramming to develop into teratomas. These results together suggest that AKT activation affects cell cycle in PGCs to enhance their reprogramming.

In other work, we suggested that downregulation of Ezh2, a tri-methyltransferase for histone H3 lysine (K) 27, and the subsequent decline of H3K27me3 in *Dnd1*-deficient germ cells in embryonic testes plays a role in the reprogramming of germ cells and teratoma development (Gu et al., 2018). We also showed that Ezh2 repressed the expression of *Ccnd1* (which encodes cyclin D1) via H3K27me3, while overexpression of *Ezh2* or knockdown of *Ccnd1* in PGCs in culture repressed their reprogramming. Those results implied that H3K27me3 represses PGC reprogramming via cell cycle control. In the present study, we studied possible linkages between AKT activation and cell cycle / H3K27me3 changes in PGC reprogramming.

Materials and methods

Collecting PGCs

The Oct4-ΔPE-GFP transgenic mice (Yoshimizu et al., 1999) were maintained in a C57BL/6J genetic background. Akt-Mer transgenic mice (Kimura et al., 2008) were maintained in the B6D2F1 genetic background or a mixed B6D2F1 / MCH genetic background; B6D2F1 and MCH mice were purchased from Japan SLC (Shizuoka, Japan). The mice were maintained and bred in an environmentally controlled and specific pathogen-free facility, the Animal Unit of the Institute of Development, Aging and Cancer (Tohoku University), according to the guidelines for handling of experimental animals defined by the facility. Animal protocols were reviewed and approved by the Tohoku University Animal Studies Committee. Noon on the day of the plug was defined as E0.5. Embryos of the indicated stages were obtained from female Akt-Mer transgenic mice mated with male Oct4-ΔPE-GEP transgenic mice. Embryos were collected and dissected in

Dulbecco's modified Eagle medium (DMEM; Thermo Fisher Scientific, Waltham, MA, USA) containing 10% fetal bovine serum (FBS). The genital ridges of E12.5 embryos were dissected from individual embryos.

Flow cytometry

Tissue samples containing PGCs, prepared as described above, were incubated for 1 h at 37°C with 1.2 mg/ml collagenase (Sigma-Aldrich, St. Louis, MO, USA) in phosphate-buffered saline (PBS) containing 10% FBS. To prepare single-cell suspensions for flow cytometry, cells were dissociated by pipetting, and samples were filtered through a 40-μm pore nylon mesh (BD Bioscience, Bedford, MA, USA). An ALTRA (Beckman Coulter, Brea, CA, USA) or S3 (Bio-Rad, Hercules, CA, USA) cell sorter was used to sort and collect PGCs with intense GFP expression.

Culture of PGCs for EGC formation

The sorted PGCs were cultured on a feeder layer of Sl/Sl4-m220 cells (Matsui et al., 1991) pre-treated with mytomycin C in 4-well tissue culture dishes with EG medium, which was based on the previously reported GSC culture medium with modifications [StemPro34 SFM containing StemPro34 Nutrient (Thermo Fisher Scientific), 100 μg/ml transferrin (Sigma-Aldrich), 2 nM L-glutamine (Thermo Fisher Scientific), 25μg/ml insulin (Sigma-Aldrich), 50 μM 2-mercaptoethanol (Sigma-Aldrich), 20 ng/ml EGF (Sigma-Aldrich), 25 ng/ml human bFGF (Sigma-Aldrich), 1×10^3 U/ml LIF (ESGRO, Merck-Millipore, Burlingtom, MA, USA), 100 U/ml penicillin-streptomycin (Sigma-Aldrich) and 10% KSR (Thermo Fisher Scientific)] (Kanatsu-Shinohara et al., 2003). After 7-9 days in culture, staining for alkaline phosphatase activity was used to identify EGC colonies, as described previously (Matsui et al., 1992). The efficiency of EGC formation was determined as a ratio of the number of EGC colonies to initially plated PGC number. 4-Hydroxytamoxifen (4OHT; Sigma-Aldrich) and 3-deazaneplanocin A hydrochloride (DZNeP; Selleck Chemicals, Houston, TX, USA) were added at 100 nM and 50 nM, respectively. For cell cycle analysis, RT-qPCR, and immunostaining, cell suspensions containing GFP-positive PGCs obtained from E12.5 embryos were cultured with or without 4OHT for 2 days.

Cell cycle analysis

The APC-BrdU Flow Kit (BD Bioscience) was used for estimating the per-cell amount of DNA. The kit was used according to the manufacturer's instructions, but cells were stained only with 7-amino-actinomycin D (7AAD). Flow cytometric analysis was performed using an FC500 unit (Beckman Coulter) and FlowJo software (BD Bioscience). The ratios of GFP-positive PGCs in

the G1/G0, S, and G2/M phases were estimated using the Dean-Jett-Fox model.

RT-qPCR

Cultured PGCs were purified by cell sorting as described above. Total RNA was purified from the sorted PGCs using an RNeasy Micro kit (Qiagen, Venlo, Netherland) and was used to synthesize cDNA. PCR was performed using Power SYBR Green master mix (Thermo Fisher Scientific) according to the manufacturer's instructions; the primers were as shown in Supplementary Table S1. PCR signals were detected by using CFX Connect (Bio-Rad). *Ppia* were used as internal controls.

Immunofluorescent staining of cultured PGCs

Cultured PGCs were purified by cell sorting, and were adhered to microscope slides coated with aminosilane (APS). The slides were air-dried for 30 min and then fixed in 4% paraformaldehyde for 15 min at room temperature. After washing with PBS, the slides were immersed in PBST (PBS containing 0.1% Triton X-100) for 15 min at room temperature, treated for 1 h at room temperature with blocking solution (PBST containing 5% BSA), and incubated overnight at 4°C with anti-Ser473-phosphorlated AKT (pAKT) (Cell Signaling; 1:50) and anti-p27 (Santa Cruz; 1:100) antibodies, or with anti-pAKT and anti-H3K27me3 (Abcam; 1:100) antibodies (diluted with the blocking solution). Cells then were washed with PBS and subsequently incubated for 1 h at room temperature in blocking solution containing 1 μg/ml DAPI along with goat anti-rabbit IgG conjugated to Alexa Fluor 488 and goat anti-mouse IgG conjugated to Alexa Fluor 568. The cells again were washed with PBS and were observed under a fluorescent microscope (Leica AF6000). Fluorescence intensity for $p27^{kip1}$ or H3K27me3 in pAKT-positive or -negative PGCs was quantitatively estimated by using Hybrid Cell Count Module in BZ-9000 and BZ-H2C (Keyence, Osaka, Japan).

Statistical analysis

Significant differences were determined using a Student's t-test. $P < 0.05$ was considered a statistically significant difference.

Results

AKT activation changes cell cycle of PGCs.

We first explored whether the cell cycle of PGCs was changed by AKT activation. We isolated GFP-positive PGCs from E12.5 embryos obtained from Akt-Mer transgenic female mice (Kimura et al., 2008) mated with Oct4-ΔPE-GFP transgenic males specifically expressing GFP in PGCs

(Yoshimizu et al., 1999) (Fig. 1A), and cultured these PGCs for 24 hr with 4-hydroxy tamoxifen (4OHT) to activate the AKT-MER protein. As a control, we also cultured E12.5 PGCs of Akt-Mer/Oct4-ΔPE-GFP transgenic embryos without 4OHT. We then analyzed the cell cycle of the cultured PGCs by flow cytometry, and found that cell cycle was significantly changed by AKT activation (Fig. 1B). AKT activation caused the ratio of PGCs in G1/G0 phase to decrease from 34% to 24% (Fig. 1C), suggesting that the G1-S transition is enhanced by AKT activation. At the same time, the ratio of PGCs in G2/M phase increased from 31% to 46% (Fig. 1C). These results suggested that the cell cycle change of PGCs is correlated with enhanced reprogramming of PGCs by AKT activation.

The expression of $p27^{kip1}$ is downregulated by AKT activation

We then examined the effect of AKT activation on expression of the CDK inhibitors $p21^{cip1}$ and $p27^{kip1}$, proteins that are known to prevent G1-S transition and likely are involved in the above-mentioned cell-cycle changes. We used RT-qPCR to test the expression of *p21*^{cip1} and *p27*^{kip1} in PGCs cultured for 48 hr with or without 4OHT. This analysis showed that the expression of *p27*^{kip1}, but not that of *p21*^{cip1}, was significantly decreased by AKT activation (Fig. 2A). Although a previous study showed that 4OHT induced *p27*^{kip1} expression (Lee et al.,1999), its expression was not significantly increased in PGCs by 4OHT (Fig. 2B). We also performed immuno-staining of cultured PGCs using antibodies against $p27^{kip1}$ and phosphorylated AKT (Ser473-pAKT). The results indicated that fluorescent intensity for $p27^{kip1}$ in the Ser473-pAKT-positive (AKT-active) PGCs was significantly lower on average, than that in the Ser473-pAKT-negative (AKT-inactive) PGCs, though the intensity was varied among the cells (Fig. 3A, B). The results together suggest that AKT activation is involved in decreased expression of $p27^{kip1}$, which may result in promotion of the G1-S transition in PGCs.

AKT activation induces hypomethylation of H3K27 in PGCs, enhancing reprogramming.

We next used immuno-staining to examine the effect of AKT activation on H3K27me3. This experiment followed from our previous demonstration that decreased H3K27me3 is involved in reprogramming PGCs to pluripotent teratoma-forming cells (Gu et al., 2018). In the present work, we examined levels of H3K27me3 by immune-staining, and found that fluorescence intensity for H3K27me3 in AKT-active PGCs was lower compared with that in AKT-inactive PGCs (Fig. 4A, B). We then investigated the effect of 3'-deazaneplanocin A (DZNeP; a known inhibitor of the H3K27 tri-methyltransferase EZH2) on formation of EGC colonies from PGCs in culture (Fig. 4C). The results showed that DZNeP alone enhanced EGC formation, though the efficiency of this effect was lower than that obtained by AKT activation. These results together suggested that AKT activation-dependent enhancement of PGC reprogramming is due in part to reduced

H3K27me3.

Discussion

Previous studies reported that AKT activation in PGCs promoted their reprogramming, an effect that may be due, at least in part, to downregulation of p53 expression (Kimura et al., 2008). Because p53 stimulates transcription of genes negatively controlling the cell cycle, including the gene encoding the CDK inhibitor $p27^{kip1}$, the present work examined the possible effects of AKT activation on cell cycle in PGCs at early stages of EGC formation. We found that the ratio of PGCs in G1/G0 was decreased (Fig.1), and the expression of $p27^{kip1}$ (both at the transcriptional and translational levels) was concomitantly down-regulated, by AKT activation (Fig.2). Functions of $p27^{kip1}$ are post-transcriptionally controlled by AKT in cancer cells, where nuclear translocation of phosphorylated $p27^{kip1}$ by AKT is repressed (Liang et al., 2002; Shin et al., 2002), while $p27^{kip1}$ expression is transcriptionally repressed by AKT via phosphorylation of a Forkhead transcription factor AFX (Medema et al., 2000). In the case of PGCs, localization of $p27^{kip1}$ was not affected, but both mRNA and protein of Akt were downregulated by AKT activation, suggesting involvement of transcriptional control of $p27^{kip1}$. $p27^{kip1}$ protein levels were varied among individual cells even without AKT activation (Fig. 3A), and it suggests that additional cell-intrinsic factors are involved in the expression of $p27^{kip1}$.

These results suggested that AKT activation promotes G1-S transition via downregulation of $p27^{kip1}$ expression. At the same time, the ratio of PGCs in G2/M was increased by AKT activation, suggesting a slowdown in the G2-M transition, though the meaning of this effect on PGC reprogramming is currently unclear. In ESCs, the G1/S check point is missing, and length of G1 phase is much shorter than that in somatic cells (Neganova and Lako, 2008). Meanwhile, the length of the G1 phase becomes longer in ESCs initiating differentiation (Kapinas et al., 2013). Differentiation generally starts in cells in the G1/G0 phase, and therefore a short G1 phase may be favorable for ESCs to maintain their undifferentiated status. Furthermore, a previous study in mouse embryonic fibroblasts (MEFs) and in granulocyte-monocyte progenitors (GMPs) demonstrated that fast-cycling cells are prone to reprogramming (Guo et al., 2014). Therefore, it is likely that a shorter G1 phase may be favorable for reprogramming. In PGCs, the shortening of the G1 phase by AKT activation may prevent differentiation of the cells and subsequent cell cycle arrest or apoptosis, which normally occur in culture; consequently, more PGCs may have a chance to undergo reprogramming.

In our previous study, we demonstrated that decreased H3K27me3 is closely correlated to conversion of germ cells into pluripotent early teratoma cells in embryonic testis, and that the H3K27 trimethytransferase EZH2 impaired the reprogramming of PGCs into pluripotent EGCs

in culture (Gu et al., 2018). In addition, EZH2 negatively regulated the expression of *Ccnd1*, a gene that encodes a protein (cyclin D1) that promotes G1-S transition. In the present study, we found that AKT activation diminished H3K27me3 in cultured PGCs, and confirmed that inhibition of EZH2 by DZNeP enhanced EGC formation (Fig.3). These results together suggested that activated AKT promotes reprogramming of PGCs by accelerating the G1-S transition by impeding the accumulation of $p27^{kip1}$ and that of H3K27me3. In cancer cells, AKT plays a role on the expression of EZH2 (Riquelme et al., 2015), but detailed mechanisms of EZH2 upregulation are unknown. Elucidation of a mechanism whereby AKT activation decreases H3K27me3 will be an important subject for future studies.

Acknowledgments

We thank all the members of Cell Resource Center for Biomedical Research for helpful discussions, and the Center of Research Instruments in the Institute of Development, Aging for use of instruments. Y.M. was supported by a Grant-in-Aid for Scientific Research (KAKENHI) in Innovative Areas, "Mechanisms regulating gamete formation in animals" (Grant #25114003), from the Ministry of Education, Culture, Sports, Science and Technology of Japan, and by a grant from AMED-CREST (Grant #JP17gm0510017h) from the Japan Agency for Medical Research and Development.

References

Abukkhdeir, A.M., Park, B.H. (2008). P21 and p27: roles in carcinogenesis and drug resistance. Expert Rev. Mol. Med. 10, e19.

Brazil, D.P., Yang, Z-Z., Hemmings, B.A. (2004). Advances in protein kinase B signaling: AKT ion on multiple fronts. Trends Biochem. Sci. 29, 233-242.

Cook, M.S., Munger, S.C., Nadeau, J.H., Capel, B. (2011). Regulation of male germ cell cycle arrest and differentiation by DND1 is modulated by genetic background. Development. 138, 23-32.

El-Deiry,W.S., Tokino,T., Velculescu,V.E., Levy,D.B., Parsons,R., Trent,J.M., Lin, D., Mercer,E., Kinzler,K.W., Vogelstein,B. (1993). *WAF1*, a potential mediator of p53 tumor suppression Cell 75, 817-825.

Ginsburg M, Snow MH, McLaren A (1990) Primordial germ cells in the mouse embryo during gastrulation. *Development* 110**:** 521-528.

Gu, W., Mochizuki, K., Otsuka, K., Hamada, R., Takehara, A., Matsui, Y. (2018). Dnd1-mediated epigenetic control of teratoma formation in mouse. Biol. Open 7, bio030106.

Guo, S., Zi, X., Schulz, V.P., Cheng, J., Zhong, M., Koochaki, S.H.J., Megyola, C.M., Pan, X., Heydari, K., Weissman, S.M., Gallagher, P.G., Krause, D.S., Fan, R., Lu, J. (2014). Non-stochastic reprogramming from a privileged somatic cell state. Cell 156, 649-662.

Kanatsu-Shinohara, M., Ogonuki, N., Inoue, K., Miki, H., Ogura, A., Toyokuni, S., Shinohara, T. (2003). Ling-term proliferation in culture and germline transmission of mouse male germline stem cells. Biol. Reprod. 69, 612-616.

Kapinas, K., Grandy, R., Ghule, P., Medina, R., Becker, K., Pardee, A., Zaidi, S.K.,Lian, J., Stein, J., Wijnen, A.V., Stein, G. (2013). The abbreviated pluripotent cell cycle. J. Cell Physiol. 228, 9-20.

Kimura, T., Tomooka, M., Yamano, N., Murayama, K., Matoba, S., Umehara, H., Kanai, Y., Nakano, T. (2008). AKT signaling promotes derivation of embryonic germ cells from primordial germ cells. Development 135, 869–879.

Lee, T.H., Chuang, L.-Y., Hung, W.-C. (1999). Tamoxifen induces $p21^{WAF1}$ and $p27^{KIP1}$ expression in estrogenreceptor-negative lung cancer cells. Oncogene 18, 4269-4274.

Liang, J., Zubovitz, j., Petrocelli, T., Kotochetkov, R., Cannor, M.K., Han, K., Lee, J-H., Ciarallo, S., Catzavelos, C., Beniston, R., Franssen, E., Slingerland, J.M. (2002). PKB/Akt phosphorylates p27, ompairs nuclear import of p27 and opposes p27-mediated G1 arrest. Nat. Med. 8, 1153-1160.

Matsui Y., Toksoz,D., Nishikawa,S., Nishikawa,S.-I., Williams,D., Zsebo,K.M. and Hogan,B.L.M. (1991) Effect of Steel factor and leukaemia inhibitory factor on murine primordial germ cells in culture. *Nature* 353: 750-752.

Matsui, Y., Zsebo,K.M. and Hogan,B.L.M.(1992). Derivation of pluripotential embryonic stem cells from murine primordial germ cells in culture. Cell 70, 841-847.

Matsui, Y., Takehara, A., Tokitake, Y., Ikeda, M., Obara, Y., Morita-Fujimura, Y., Kimura, T., and Nakano, T. (2014). The majority of early primordial germ cells acquire pluripotency by Akt activation. Development 141, 4457-4467.

Medema, R.H., Kops, G.J.P.L., Bos, J.L., Burgering, B.M.T, (2000). AFX-like Forkhead transcrittion factors mediate cell-cycle regu;ation by Ras and PKB through $p27^{kip1}$. Nature 404, 782-787.

Neganova, I., Lako, M. (2008). G1 to S phase cell cycle transition in somatic and embryonic stem cells. J.Anat. 213, 30-44.

Riquelme, E., Behrens, C., Lin, H.Y., Simon, G., Papadimitrakopoulou, V., Izzo1, J., Moran, C., Kalhor, N., Lee, J.J., Minna, J.D., Wistuba, I.I. (2016). Modulation of EZH2 Expression by MEK-ERK or PI3K-AKT Signaling in Lung Cancer Is Dictated by Different KRAS Oncogene Mutations. Cancer Res. 76, 675-685.

Resnick, J.L., Bixler, L.S., Cheng, L., and Donovan, P.J. (1992). Long-term proliferation of mouse primordial germ cells in culture. Narure 359, 550-551

Shin, I., Yakes, F.M., Rojo, F., Shin, N-Y., Bakin, A.V., Baselga, J., Arteaga, C.L. (2002). PLG/Akt mediates cell-cycle progression by phosphoprylation of $p27^{kip1}$ at threonine 157 and modulation of its cellular localization. Nat.Med. 8, 1145-1152.

Stevens, L.C. (1973). A new inbred subline of mice (129-terSv) with a high incidence of spontaneous congenital testicular teratomas. J. Natl. Cancer Inst. 50, 235-242.

Yoshimizu, T., Sugiyama, N., De Felice, M., Yeom, Y.I., Ohbo, K., Masuko, K., Obinata, M., Abe, K., Schöler, H.R., Matsui, Y. (1999). Germline-specific expression of the Oct-4/green fluorescent protein (GFP) transgene in mice. Dev. Growth Differ. 41, 675-684.

Figure legends

Figure 1. The effect of AKT activation on cell cycle in PGCs.

(A) Gating of GFP-positive PGCs on flow cytometry for cell cycle analysis. Right panel shows cultured genital ridge cells of Akt-Mer × Oct4-ΔPE-GFP transgenic embryos at E12.5; left panel shows the equivalent from Akt-Mer × B6D2F1 transgenic embryos (used as a negative control

for GFP expression). (B) Cell cycle of GFP-positive PGCs cultured with or without 4OHT was examined by flow cytometry. The cells were stained with 7-amino-actinomycin D (7AAD) to permit estimation of the amount of DNA in the cells. (C) The percentage of PGCs in the G1/G0, S, and G2/M phases. The data are presented as the mean±s.e.m. of four independent experiments. *p<0.05; **p<0.001 (Student's t test).

Figure 2. Down-regulation of $p27^{kip1}$ mRNA by AKT activation in PGCs.

(A) The expression of *p21*^{cip1} and *p27*^{kip1} in E12.5 PGCs obtained from Akt-Mer × Oct4-ΔPE-GFP transgenic embryos, and cultured with or without 4OHT for 2 days. (B) The expression of *p27*^{kip1} in E12.5 PGCs obtained from MCH × Oct4-ΔPE-GFP transgenic embryos, and cultured with or without 4OHT for 2 days. GFP-positive PGCs were purified after culturing, and transcript levels were determined by RT-qPCR. *Ppia* were used as internal controls. The expression levels in PGCs cultured without 4OHT were set as 1.0. The data are presented as the mean±s.e.m. of three independent experiments. *p<0.05 (Student's t test).

Figure 3. Down-regulation of $p27^{kip1}$ protein by AKT activation in PGCs.

(A) The expression of $p27^{kip1}$ protein in PGCs cultured with 4OHT for 2 days. PGCs were purified after culture, and were stained with antibodies against the Ser473-phosphorylated AKT (pAKT; green) and $p27^{kip1}$ (red), as well as with DAPI (blue). White arrowheads indicate pAKT signal. Scale bars: 10 μm. (B) Quantitative estimation of fluorescence intensity for $p27^{kip1}$ in pAKT-positive or -negative PGCs in a given field; 10 different fields were observed and fluorescence intensity of 30-200 cells in each field was measured in each experiment. The fluorescence intensities in pAkt- PGCs were set as 1.0. The data are presented as the mean±s.e.m. of three independent experiments. *p<0.05 (Student's t test).

Figure 4. Decreased H3K27 methylation following AKT activation in PGCs.

(A) H3K27me3 in E12.5 PGCs cultured with 4OHT for 2 days. PGCs were purified after culturing, and were stained with the antibodies against pAKT (green) and H3K27me3 (red), as well as with DAPI (blue). White arrowheads indicate pAKT signal. Scale bars: 10 μm. (B) Quantitative estimation of fluorescence intensity for H3K27me3 in pAKT-positive or -negative PGCs in a given field; 10 different fields were observed and fluorescence intensity of 30-200 cells in each field was measured in each experiment. The fluorescence intensities in pAkt- PGCs were set as 1.0. (C) The effect of DZNeP, a specific inhibitor of the H3K27 methyltransferase EZH2, on the reprogramming of PGC to EGCs. Purified E12.5 PGCs were cultured with or without 4OHT and DZNeP; 4OHT and DZNeP were added for the initial 2 days in culture. The efficiency of reprogramming is represented by ratios of EGC colony number to initially plated PGC number.

The data are presented as the mean±s.e.m. of three (B) or four (C) independent experiments. *p<0.05 (Student's t test).

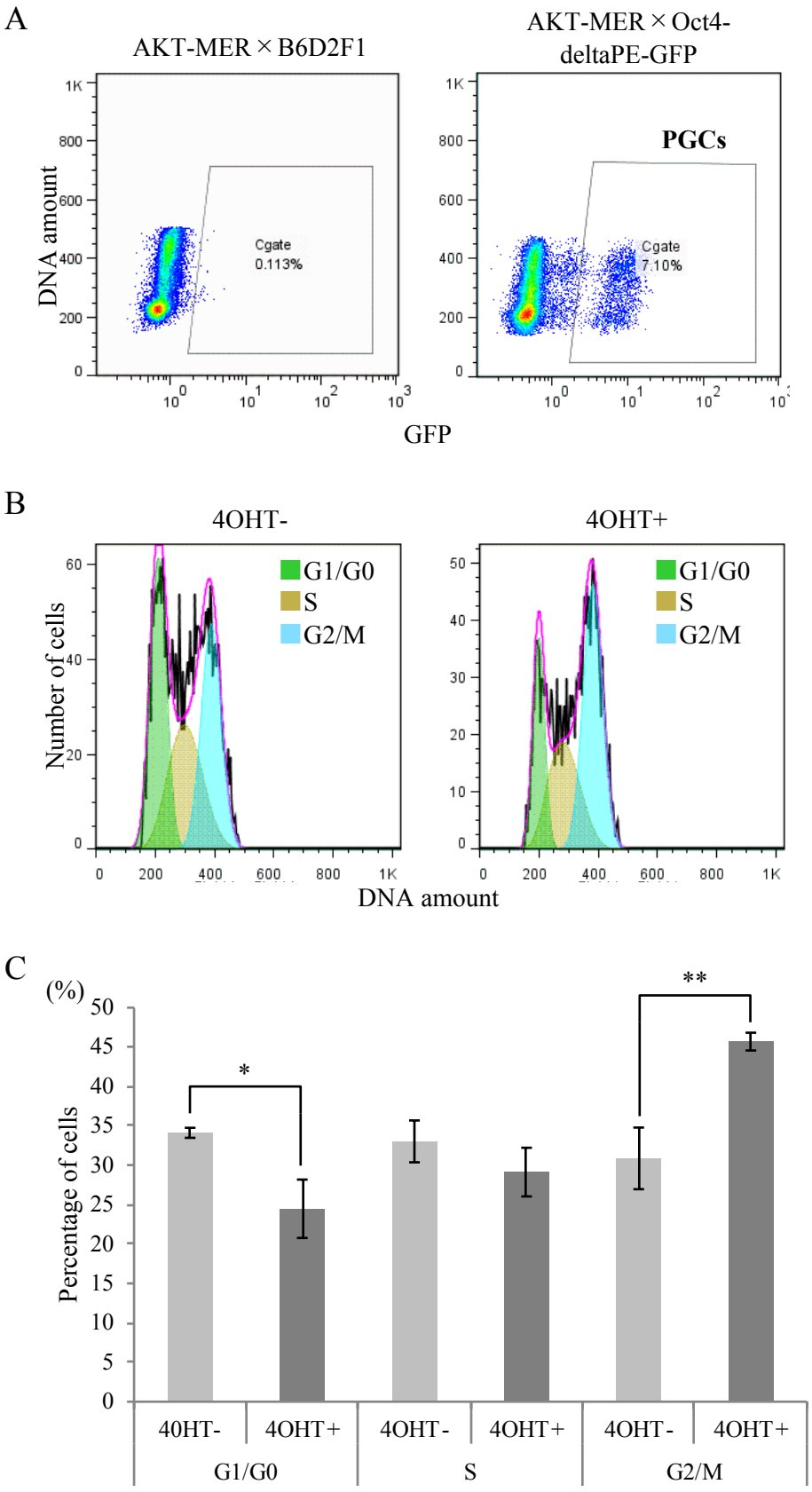
A
AKT-MER × B6D2F1
AKT-MER × Oct4-deltaPE-GFP
PGCs
Cgate 0.113%
Cgate 7.10%
DNA amount
GFP
B
4OHT-
4OHT+
G1/G0
S
G2/M
Number of cells
DNA amount
C
(%)
Percentage of cells
*
**
40HT-
4OHT+
4OHT-
4OHT+
4OHT-
4OHT+
G1/G0
S
G2/M

Figure 1

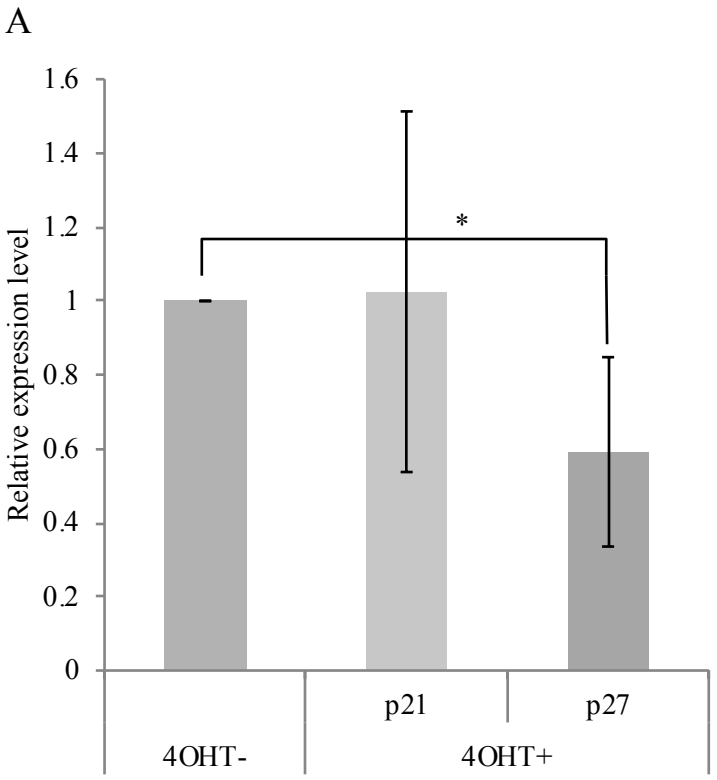
A
1.6
1.4
1.2
1
0.8
0.6
0.4
0.2
0
Relative expression level
*
p21
p27
4OHT-
4OHT+

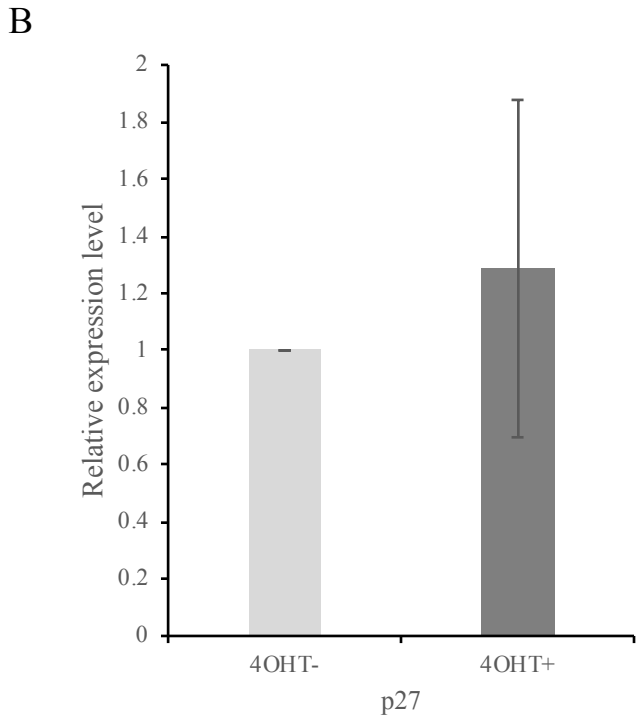
B
2
1.8
1.6
1.4
1.2
1
0.8
0.6
0.4
0.2
0
Relative expression level
4OHT-
4OHT+
p27

Figure 2

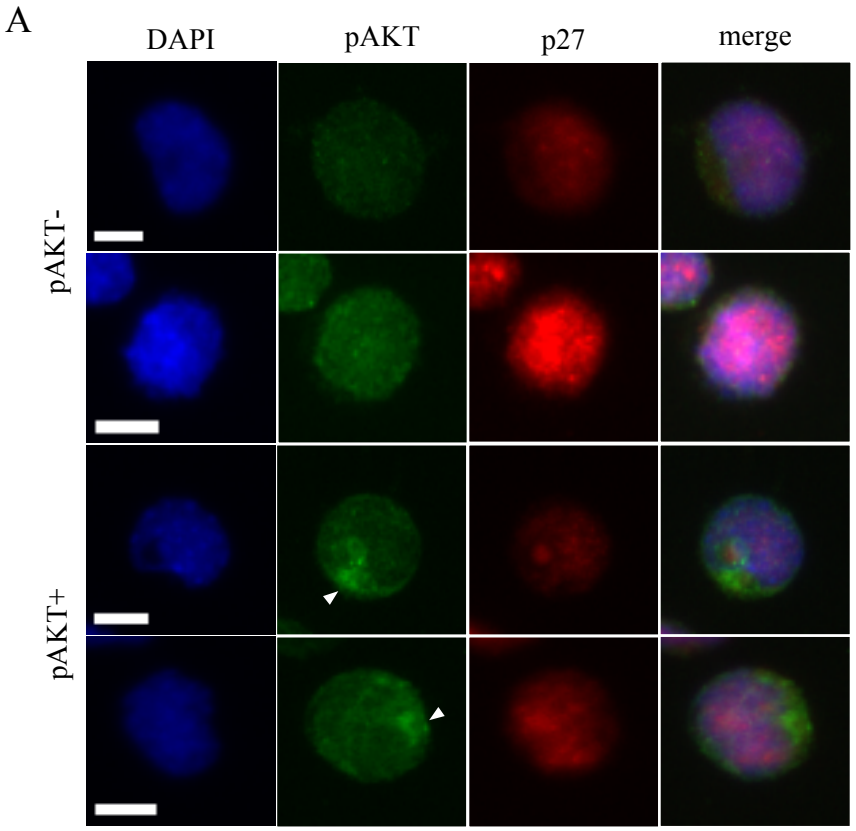
A
DAPI
pAKT
p27
merge
pAKT-
pAKT+

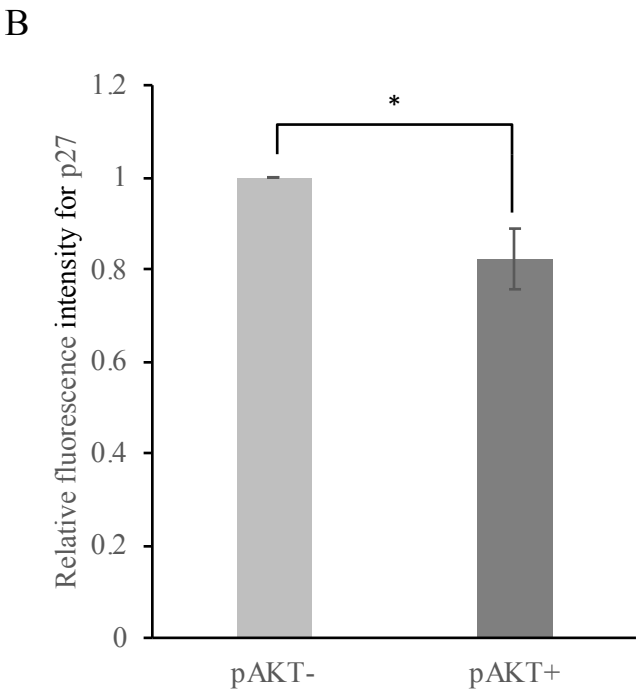
B
Relative fluorescence intensity for p27
1.2
1
0.8
0.6
0.4
0.2
0
*
pAKT-
pAKT+

Figure 3

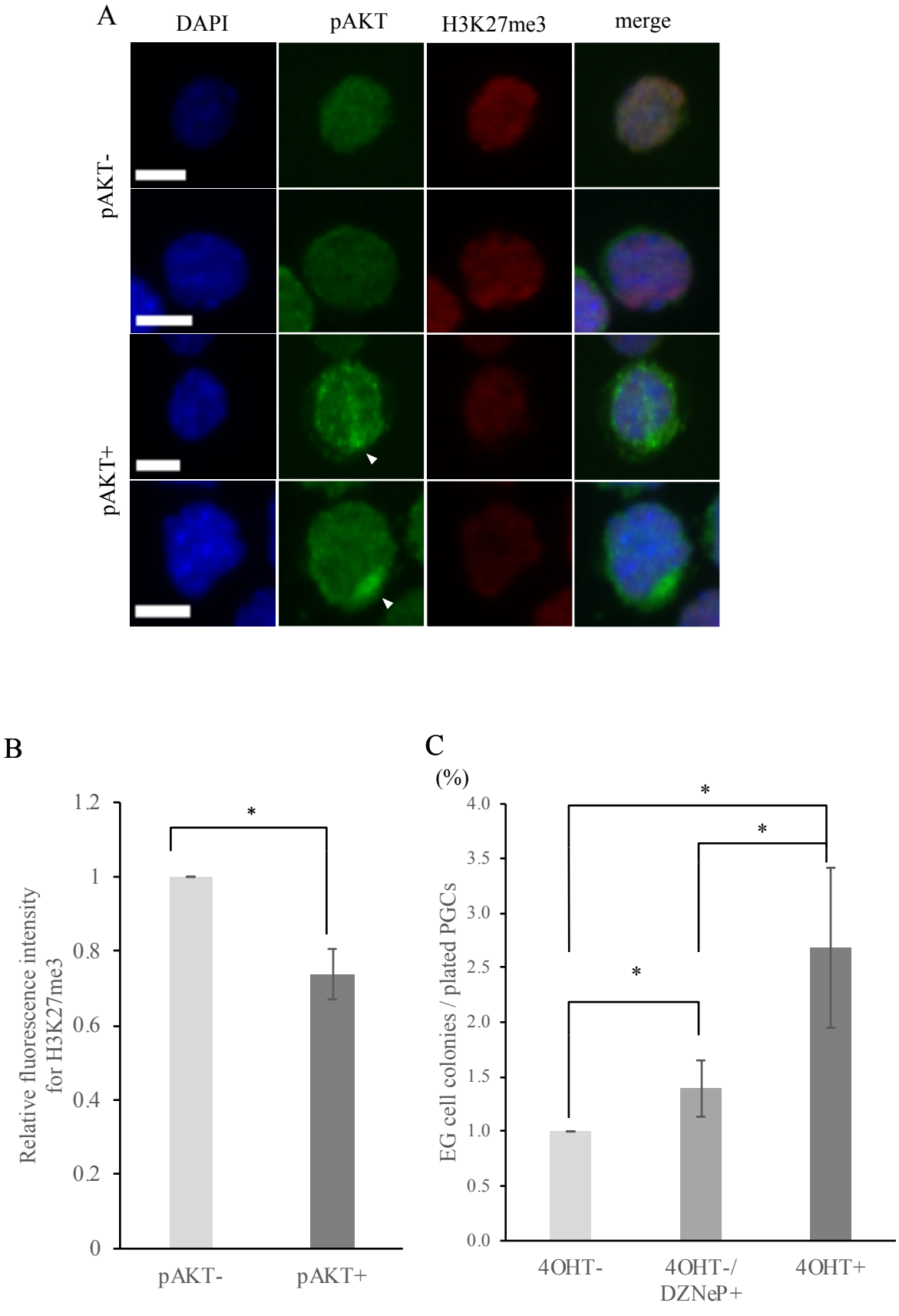
A
DAPI
pAKT
H3K27me3
merge
pAKT-
pAKT+
B
Relative fluorescence intensity for H3K27me3
1.2
1
0.8
0.6
0.4
0.2
0
*
pAKT-
pAKT+
C
(%)
EG cell colonies / plated PGCs
4.0
3.5
3.0
2.5
2.0
1.5
1.0
0.5
0.0
*
*
*
4OHT-
4OHT-/ DZNeP+
4OHT+

Figure 4